

Correct patient centering increases image quality without concomitant increase of radiation dose during adult intracranial computed tomography

Al Mohiy H^{1*}; Emad Alasar 2* and Charbel Saade ^{3*}

¹⁻²Department of Radiological Science, King Khalid University, Abha, Saudi Arabia.

^{3*}Department of Diagnostic Radiology, American University of Beirut Medical Center, Lebanon

Abstract

Purpose: To evaluate the impact of patient centering and radiation dose during intracranial computed tomography (ICT) on quantitative and qualitative image quality.

Materials and Methods: 500 consecutive patients who underwent ICT were retrospectively reviewed using a 128-slice CT scanner (Definition AS+, Siemens, Germany). Patients were subjected in equal numbers to one of two positioning protocols: Group A, poorly centered; and Group B, involved accurate centering prior to imaging. Gray-white matter (GWM) conspicuity, contrast-to-noise (CNR), and signal-to-noise (SNR) in each group were calculated. Qualitative image quality in terms of GWM differentiation, distinctness of posterior fossa contents, and overall diagnostic acceptability were evaluated by two neuroradiologists. The dose length product (DLP), CNR, SNR, and noise were measured between each group and data generated were compared using Mann-Whitney U non-parametric statistics. Visual grading characteristic (VGC) and kappa analyses were performed.

Results: The mean noise index was significantly lower in group B (2.61 ± 0.29) compared to A (2.66 ± 0.21) ($p < 0.02$). The mean attenuation of GWM, SNR, and CNR in the frontal lobe (A; $1:0.77, 0.84, 8.70 \pm 1.36$ and B; $1:0.65, 0.85, 15.32 \pm 1.21$) ($p < 0.02$), occipital lobe (A; $1:1.10, 1.18, 10.79 \pm 2.11$, and B; $1:0.94, 0.64, 14.41 \pm 3.09$) ($p < 0.04$), and cerebellum (A; $1:0.79, 0.90, 12.56 \pm 4.08$ and B; $1:0.82, 0.87, 14.07 \pm 2.28$) ($p < 0.04$) were significantly higher in group B compared to A, while the globus pallidus, caudate nucleus, and optic track in the basal ganglia demonstrated no difference in each group ($p > 0.05$). Mean DLP demonstrated no significance between each group (A: 1312.03 ± 133.92 , B: 1298.11 ± 130.61). The qualitative analyses demonstrated significant increases in VGC for each reader ($p < 0.02$) and inter-observer agreement was significantly increased in protocol B ($k = 0.81$) compared to A ($k = 0.62$).

Conclusion: Correct patient centering increases the CNR and SNR in both GWM in the left and right hemispheres of the brain during ICT.

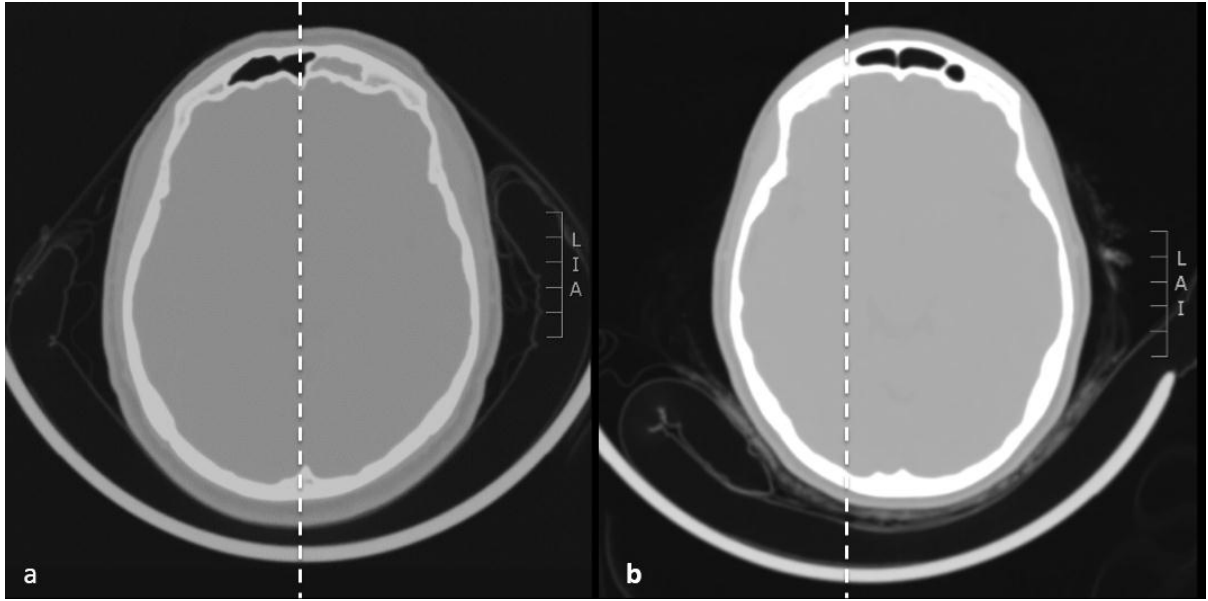


Figure 1. Optimal head centering (a) and sub-optimal head centering (b) during intracranial CT.

Quantitative image analysis

A neuroradiologist certified by the American Board of Radiology and with seven years' experience assessed the images. For all axial reconstructions, 4 mm circular and two regions of interest (ROI) are placed in corresponding white matter (WM) and gray matter (GM) locations (at the level of the basal ganglia) as well as in the pons (these are common areas of stroke prevalence). Signal was defined as CT density in Hounsfield Units (HU), and image noise as standard deviation (SD) of attenuation within a ROI. SNR and CNR were calculated using the following standard equations [20]:

$$SNR = \frac{\text{mean HU of tissue in ROI}}{SD \text{ of HU in ROI}}$$

$$CNR = \frac{\text{mean GM HU} - \text{mean WM HU}}{\sqrt{[(SD \text{ GM HU})^2 + (SD \text{ WM HU})^2]}}$$

analyses studies (ordinal ratings). In VGC analysis, plotting the visual grading analyses data of A versus B in a manner similar to that used in ROC analysis assessed the relative performance of pathology detection and image quality. The resulting measure of image quality is the VGC curve, which describes the relationship between the proportions of fulfilled image criteria for the two compared conditions. Subjective image quality will be assessed on axial datasets in terms of noise, grey-white matter differentiation, distinctness of posterior fossa contents, and overall diagnostic acceptability. Noise was graded as 1=very low, 2=low, 3=considerable with preserved diagnostic image quality, and 4=high and causative to non-diagnostic image quality. All other parameters were scored as 1=excellent, 2=good, 3=suboptimal but still diagnostic, and 4=unacceptable and non-diagnostic. Grades for image quality were averaged across both readers for further analysis.

The inter- and intra-observer agreements were calculated using Cohen's kappa analysis. A k value of 0.60–1, 0.41–0.60, 0.21–0.40, and less than 0.20 was considered excellent, moderate, fair, and poor agreement, respectively.

Statistical analysis

Statistical analysis was performed with software (JMP version 6, SAS Institute, Cary, NC; Prism version 4.00, Graph Pad Software, San Diego, CA). A p value of less than 0.05 indicated statistical significance. Unpaired t-test and Chi-square test were used to compare continuous and proportional patient characteristics between the two groups. Comparison of quantitative image quality parameters in axial reconstructions with measurements in standard dose was performed by unpaired t-test. Mann Whitney test was used for comparison of subjective image quality scores. Inter-rater agreement in the assessment of image quality was quantified by weighted kappa statistics [22].

Basal ganglia, pons and optic tract

The mean attenuation (HU) of the globus pallidus, caudate nucleus, and optic tract in the basal ganglia demonstrated no difference in attenuation values in each group. The pons demonstrated no significant difference between the left and right side of the pons in each group (Table 6).

Table 6: Anatomical measurements of the basal ganglia, pons and optic tract.

Anatomy Location	HU		HU		P value
	Group A	SNR	Group B	SNR	
Basal Ganglia					
Globus Pallidus	33.28 ±	11.41 ±	33.17 ±	10.33 ±	0.803
Caudate	2.49	1.15	2.46	1.17	0.102
Nucleus	34.89 ±	12.10 ±	26.89 ±	11.19 ±	
Pons	2.07	2.03	2.39	2.33	0.091
Right Side					0.110
Left Side	27.99 ±	9.64 ± 2.48	27.48 ±	9.64 ±	
	2.63	10.77 ±	1.73	2.48	0.683
Optic Tract	29.00 ±	3.18	28.00 ±	11.32 ±	
	2.65		2.65	2.11	
		10.79 ±			
	40.49 ±	1.56	41.10 ±	11.03 ±	
	3.79		1.47	1.86	

Note – Data are mean ± standard deviation

Radiation dose

The mean CTDI_{vol} (specifies the radiation intensity used to perform a specific CT examination) in protocol A (84.58 ± 9.89 mGy) and protocol B (82.38 ± 7.43 mGy), and the mean DLP (amount of radiation = intensity × scan length) in protocol A (1312.03 ± 133.92 mGy·cm) and B (1298.11 ± 130.61 mGy·cm) demonstrated no significant difference between

demonstrated that the optimal separation between the GWM interfaces was well below the DRL for intracranial CT with the CNR being the most accurate measurement in measuring optimal image quality between the gray and white matter in Group B ($p < 0.04$).

There are limitations to our study. First, we did not perform a comparison between filtered back projection and iterative reconstruction on the same group of patients because it would be inappropriate to expose children and adults to unnecessary radiation; rather, we preferred to compare the means of different patient groups. Second, as the quality of the examination was the focus of the study, we did not compare all of the CT findings and assess the diagnostic accuracy.

Conclusion

In conclusion, we found that correct patient centering increases the contrast and signal in both gray and white matter on the right and left hemispheres of the brain during intracranial computed tomography.

17. Paolicchi F, Faggioni L, Bastiani L, Molinaro S, Puglioli M, Caramella D, et al. Optimizing the Balance Between Radiation Dose and Image Quality in Pediatric Head CT: Findings Before and After Intensive Radiologic Staff Training. *American Journal of Roentgenology*. 2014;202(6):1309-15.
18. Goo HW. CT radiation dose optimization and estimation: an update for radiologists. *Korean J Radiol*. 2012;13(1):1-11.
19. Christner JA, Kofler JM, McCollough CH. Estimating effective dose for CT using dose-length product compared with using organ doses: consequences of adopting International Commission on Radiological Protection publication 103 or dual-energy scanning. *AJR Am J Roentgenol*. 2010;194(4):881-9.
20. Mullins ME, Lev MH, Bove P, O'Reilly CE, Saini S, Rhea JT, et al. Comparison of Image Quality Between Conventional and Low-Dose Nonenhanced Head CT. *American Journal of Neuroradiology*. 2004;25(4):533-8.
21. Bath M, Mansson LG. Visual grading characteristics (VGC) analysis: a non-parametric rank-invariant statistical method for image quality evaluation. *Br J Radiol*. 2007;80(951):169-76.
22. Viera AJ, Garrett JM. Understanding interobserver agreement: the kappa statistic. *Fam Med*. 2005;37(5):360-3.
23. Trattner S, Pearson GD, Chin C, Cody DD, Gupta R, Hess CP, et al. Standardization and optimization of CT protocols to achieve low dose. *J Am Coll Radiol*. 2014;11(3):271-8.